Developing Wear Equation for AA2024 Hybrid Composites Sliding Under Dry and Lubricating Condition

Yashwanth Kumar MADDI^{1*}, Vijaya Kumar TADIKONDA¹, Dhanasekaran RAJAGOPAL²

¹ Department of Mechanical Engineering, Koneru Lakshmaiah Education Foundation, Guntur, Andhra Pradesh, India ² Department of Mechanical Engineering, Adhiyamaan College of Engineering, Hosur Tamil Nadu, India

http://doi.org/10.5755/j02.ms.40311

Received 28 January 2025; accepted 6 March 2025

This study investigates the wear behavior of AA2024 hybrid composites reinforced with silicon carbide (SiC) and graphite (Gr) particles under both dry and lubricated conditions. Using the stir casting technique, composites with varying reinforcement percentages were fabricated and subjected to wear tests on a pin-on-disk tribometer. Parameters such as load, sliding velocity, temperature, and sliding distance were varied to evaluate their influence on wear performance. The results indicated that increasing the reinforcement percentage improves hardness and wear resistance due to enhanced load distribution and reduced thermal degradation. Under dry conditions, abrasive and adhesive wear mechanisms dominated, with mechanically mixed layers (MMLs) forming at moderate loads, reducing wear. At higher loads and sliding speeds, wear increased due to reinforcement detachment and thermal softening of the matrix. In contrast, lubrication significantly reduced wear rates by forming protective tribo-films that stabilized particle distribution and minimized friction. Scanning electron microscopy (SEM) revealed smoother surfaces and reduced wear debris under lubricated conditions, emphasizing the role of lubrication in mitigating wear. A wear equation was developed to predict wear rates under varying conditions with a strong correlation to experimental data. The findings highlight the potential of SiC and Gr reinforced AA2024 hybrid composites for applications requiring superior wear resistance under diverse operational environments.

Keywords: hybrid composites, wear equation, lubrication, microstructure, stir casting.

1. INTRODUCTION

Aluminum matrix composites are highly desired in the aerospace and automotive industries due to their exceptional properties [1]. These include a high strength-to-weight ratio, specific strength, ductility, corrosion resistance, thermal stability, and a low coefficient of thermal expansion [2]. However, one of the main challenges with aluminum composites lies in their poor wear resistance [3]. This limitation restricts their usability in structural and sliding components, which are essential in industrial operations, particularly in machine elements [4, 5]. Wear, characterized by the removal of surface material due to mechanical contact, poses a significant obstacle in achieving optimal performance [6-8]. The wear behavior of aluminum composites is influenced by factors such as the type of reinforcement, applied load, volume fraction, and sliding speed [9]. Moreover, the wear phenomena differ in dry and lubricating atmospheres, further impacting the overall performance of these composites [10]. Dry conditions increase friction and heat generation, leading to accelerated wear, while lubrication introduces protective films that reduce friction and wear [11]. Steels and titanium alloys demonstrate increased wear rates and potential for oxidation in dry conditions, forming oxide layers that can either increase friction or provide limited wear resistance depending on the environment and test duration [12]. Conversely, lubricated conditions, particularly with engine oils, show a marked reduction in both friction and wear [13]. Engine oils contain viscosity-modifying agents and antiwear additives like zinc dialkyldithiophosphate (ZDDP), which create a protective film on the contact surfaces, mitigating direct metal-to-metal contact and minimizing frictional heat generation [14]. Higher-viscosity oils form thicker films that better separate surfaces under load, contributing to improved wear resistance [15]. In lubricated conditions, ceramics, which are typically brittle and prone to microcracking under dry sliding, perform more reliably, with lubricants reducing contact stresses that lead to material loss [16]. Polymers, while exhibiting less friction under both dry and lubricated conditions due to their low hardness, show considerable improvement in wear resistance with engine oil, as it prevents thermal degradation and softening [17, 18]. The effectiveness of lubrication is determined by the film thickness and the prevailing lubrication regime, with hydrodynamic lubrication offering superior protection [19-21]. While aluminum composites reinforced with ceramics SiC and Gr have shown potential for enhanced wear resistance, several critical areas remain unexplored. Most existing studies lacks investigation on interactions between reinforcement particles, lubrication, and wear mechanisms, leading to gaps in predicting wear behavior under varying operating conditions. This research aims to develop an empirical wear equation for AA2024 hybrid composites reinforced with SiC and Gr under dry and lubricated conditions, providing a predictive framework for wear performance based on key operational parameters.

^{*} Corresponding author: Y.K. Maddi E-mail: yashwanth.gnits@gnits.ac.in

2. EXPERIMENTAL PROCEDURE

The research methodology of the proposed work was depicted in Fig. 1.

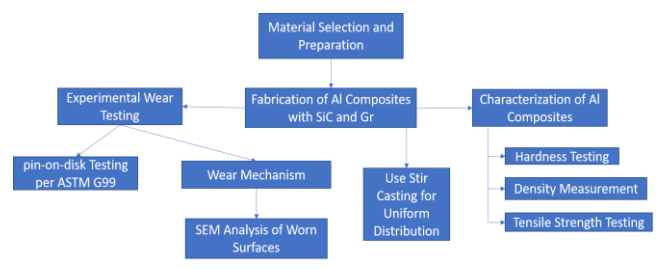


Fig. 1. Research methodology of the work

The AA2024 alloy was purchased from the Coimbatore metal mart and reinforcement particles SiC and Gr were purchased from the firm Bhukhanwala Industries, Mumbai. Aluminum composites reinforced with particles like SiC and Gr are fabricated through techniques such as stir casting to ensure even distribution of reinforcement materials [22]. The stir casting technique was employed to ensure uniform distribution of reinforcement particles within the aluminum matrix. During the stir casting process, the reinforcement particles were preheated to eliminate moisture, while the aluminum alloy was heated to a semi-solid state (approximately 600-700 °C). The preheated SiC and Gr particles were then introduced into the molten aluminum under constant stirring to achieve even distribution [23]. The resulting composite mixture was cast into molds and allowed to cool, after which specimens were prepared for wear testing according to pin-on-disk testing requirements. Hardness tests were conducted using a Rockwell hardness tester (HRB scale) following ASTM E18 standards. AA2024-SiC-Gr composite specimens were polished to ensure a smooth testing surface. A steel ball indenter (1/16inch diameter) was used with a preload of 10 kg and a major load of 100 kg. Each sample was tested at five different locations, and the average hardness value was recorded. Tensile strength tests were conducted using a universal testing machine (UTM, 50 kN capacity) following ASTM E8/E8M standards. Dog-bone-shaped specimens were machined from AA2024-SiC-Gr composites using wire electrical discharge machining (Wire-EDM) to minimize residual stresses. Wear testing was performed using a pinon-disk apparatus following ASTM G99 standards. Various operational conditions were simulated by adjusting reinforcement percentages (0.0 %, 2.5 %, 5.0 %, 7.5 %, 10.0 %), testing temperature, applied load (10 N, to 50 N), sliding velocity, and distance [24]. The wear results for are depicted in Table 1. Each composite specimen was subjected to the pin-on-disk test, where it was positioned in contact with a rotating disk. Wear rate, frictional force, and other relevant parameters were recorded for each test condition, providing insight into the wear resistance of the composite under different conditions. After wear testing, the worn surfaces of the samples were analyzed to determine the underlying wear mechanisms. Scanning Electron Microscopy (SEM) (EVO 15, ZEISS) were used to examine the wear scars and elemental composition on the worn surfaces [25]. A comprehensive data analysis was performed to evaluate the impact of various factors on wear performance.

Table 1. Wear experimental runs and its results

Run No	Reinforcement, %	Temperature, °C	Load, N	Velocity, m/s	Distance, m	Wear rate, mm³/min	Wear-lubricated, mm³/min
1	0	25	10	2	1000	0.00006	0.000122
2	0	50	20	4	2000	0.00011	0.000151
3	0	75	30	6	3000	0.00017	0.000228
4	0	100	40	8	4000	0.00035	0.000231
5	0	125	50	10	5000	0.0003	0.000305
6	2.5	25	20	6	4000	0.00009	0.000037
7	2.5	50	30	8	5000	0.00015	0.000096
8	2.5	75	40	10	1000	0.00021	0.000129
9	2.5	100	50	2	2000	0.00027	0.000169
10	2.5	125	10	4	3000	0.00028	0.000206
11	5	25	30	10	2000	0.00009	0.00003
12	5	50	40	2	3000	0.00011	0.000066
13	5	75	50	4	4000	0.00024	0.000126
14	5	100	10	6	5000	0.00029	0.000161
15	5	125	20	8	1000	0.00037	0.000147
16	7.5	25	40	4	5000	0.00014	0.000082
17	7.5	50	50	6	1000	0.00017	0.00011
18	7.5	75	10	8	2000	0.00029	0.000177
19	7.5	100	20	10	3000	0.00044	0.000166
20	7.5	125	30	2	4000	0.00052	0.000229
21	10	25	50	8	3000	0.000082	0.000125
22	10	50	10	10	4000	0.000101	0.000152
23	10	75	20	2	5000	0.000153	0.000195
24	10	100	30	4	1000	0.000205	0.000133
25	10	125	40	6	2000	0.000306	0.000232

3. RESULTS AND DISCUSSION

3.1. Microstructure

The microstructural analysis in Fig. 2, reveals that the reinforcements within the composite material appear to be well-dispersed.

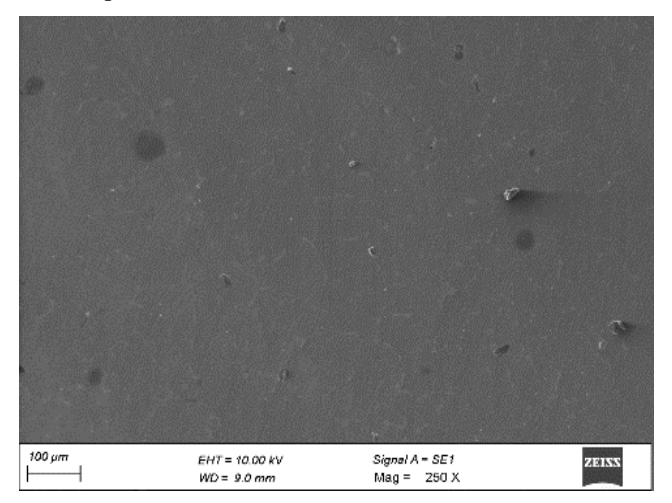


Fig. 2. SEM of AA2024 aluminum hybrid composites

The uniformity of reinforcement distribution plays a key role in ensuring that the mechanical properties of the composite are consistent throughout the material. No large clusters or agglomerations of reinforcement particles are observed, suggesting that the reinforcement phase is effectively dispersed within the matrix. The image shows a relatively smooth surface with minimal visible voids which indicated that the stir casting was effective in minimizing air entrapment. The microstructure also appears to show good bonding between the matrix and reinforcement phases. The fine-scale distribution of the reinforcements suggests that the matrix has been adequately processed to ensure a strong interface with the reinforcement particles. The addition of SiC significantly enhances the hardness of the composite by restricting grain growth and acting as a load-bearing phase, thereby improving wear resistance. In contrast, Gr particles contribute to tribological performance by forming a protective lubricating layer, reducing direct metal-to-metal contact.

3.2. Hardness

The hardness values of aluminum composites reinforced with varying percentages were observed to increase consistently with the increasing reinforcement content as shown in Fig. 3.

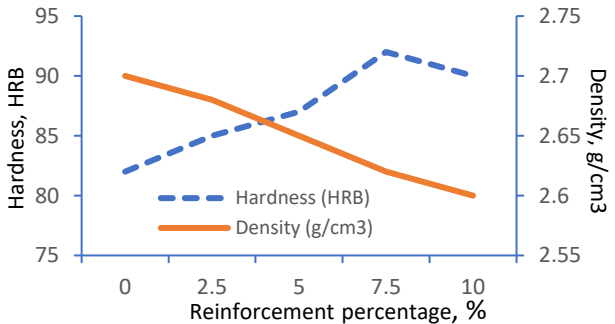


Fig. 3. Hardness and density of AA2024 hybrid composites

The increase in hardness with the rise in reinforcement percentage can be attributed to the reinforcing particles, which are harder than the aluminum matrix. The presence of these particles enhances the overall resistance to deformation and increases the material's ability to withstand external forces. This increase in hardness can be explained through the dispersion hardening mechanism, where the reinforcement particles, which are typically much harder than the aluminum matrix, restrict the movement of dislocations. This reduces the material's overall plasticity and increases its resistance to indentation. The higher density of the individual particles, the volume fraction of these particles within the composite material remains relatively small compared to the matrix material, resulting in a slight decrease in the overall composite density. Where increasing the volume fraction of reinforcement particles with lower density than the matrix leads to a reduction in the overall density of the composite material.

3.3. Tensile strength

The enhancement in tensile strength can be attributed to the reinforcement strengthening mechanism as depicted in Fig. 4. The harder reinforcement particles inhibit dislocation movement within the aluminum matrix, increasing the resistance to tensile deformation.

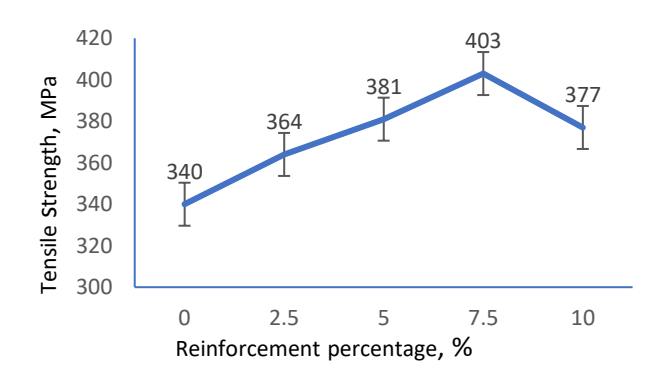


Fig. 4. Tensile strength of AA2024 hybrid composites

This phenomenon, known as dispersion hardening, occurs as the reinforcing particles create barriers to dislocations, thereby strengthening the composite. As the reinforcement content increases, the number of these barriers increases, leading to improved overall strength. The strong interfacial bonding between the aluminum matrix and the reinforcement particles further enhances the tensile properties, ensuring that the particles contribute to the strength of the composite rather than being ineffective under stress [42]. However, the rate of increase in tensile strength may eventually plateau at higher reinforcement percentages, as the matrix might become saturated with reinforcement particles, and excessive reinforcement could lead to agglomeration between particles and the matrix.

3.4. Wear rate

Reinforcements SiC and Gr possess higher hardness than the aluminum matrix, and as their concentration increases, the composite's hardness and load-bearing capacity improve as shown in Fig. 5. These ceramic particles strengthen the material, allowing it to withstand abrasive forces and resist plastic deformation [26]. This

increase in surface hardness significantly reduces the wear rate by creating a surface that is less prone to scratching or material loss during sliding interactions. As reinforcement content increases, the ceramic particles help distribute loads more effectively, reducing localized stresses within the aluminum matrix. Another contributing factor to the reduction in wear rate at higher reinforcement levels is the decreased surface adhesion and friction. The ceramic particles reduce the metal-to-metal contact area between the aluminum composite and the counterface material, lowering the COF and reducing the generation of heat during sliding. With less heat generation, thermal softening of the aluminum matrix is minimized, allowing the material to maintain wear resistance even under high loads and temperatures. Moreover, the ceramic particles act as barriers to adhesion, preventing aluminum from sticking to the counterface and reducing the extent of adhesive wear. In addition, increased reinforcement content helps in minimizing debris formation, which can create a "third body" that accelerates wear through abrasive actions. By reducing the amount of wear debris and creating a more stable wear surface, higher reinforcement levels can limit matrix erosion. This effect is particularly beneficial in dry sliding conditions where debris a significant role in surface wear. In some cases, wear debris from the ceramic particles forms a mechanically mixed layer (MML) on the composite surface, further protecting the matrix by acting as a semilubricating buffer. The wear mechanism also stabilizes at higher reinforcement percentages, shifting from severe adhesive wear to a more controlled mild abrasive wear process [27]. The hardness and rigidity provided by the reinforcement particles make the matrix less susceptible to plastic deformation and adhesion. This leads to improved long-term wear resistance, which is especially valuable in applications involving continuous cyclic loading. The increased thermal stability provided by the ceramic reinforcements also helps mitigate temperature-induced softening, as the particles dissipate frictional heat and prevent localized overheating in the matrix.

Increase in wear rate is the matrix softening at higher temperatures. As the temperature increases, the aluminum matrix becomes softer and more prone to plastic deformation under load. At higher temperatures, the aluminum matrix loses its rigidity, making it more susceptible to wear mechanisms such as abrasion and adhesion. The softened matrix can more easily deform, leading to increased material loss as the surface yields more readily under sliding contact [28]. This explains the observed rise in wear rate as temperature increases from 10 °C to 50 °C. Another contributing factor is the weakened bond between the matrix and reinforcement at elevated temperatures. High temperatures can negatively affect the interface between the aluminum matrix and the ceramic reinforcements (such as SiC or Gr). The thermal expansion mismatch between the matrix and reinforcement particles can weaken this bond, causing the reinforcement particles to become dislodged more easily [29]. When these particles detach, they no longer provide their wear-resistance benefits, which leads to a combination of abrasive and adhesive wear, further increasing the wear rate. Oxidation effects a significant role in wear behavior at elevated temperatures. As the temperature rises, oxidation on the surface of the composite increases, forming brittle oxide layers that can easily break away during sliding. These oxide particles can act as abrasive agents, similar to sandpaper, accelerating wear by introducing additional abrasive forces between the sliding surfaces. This process further contributes to the increased wear rate at higher temperatures.

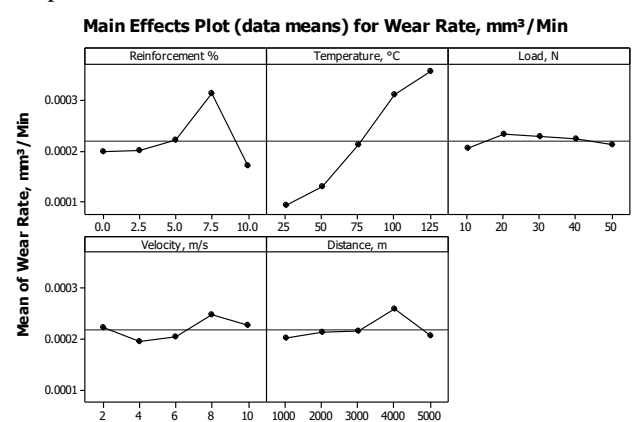


Fig. 5. The variation of wear rate in dry condition

As the applied load increases, the contact pressure at the interface between the composite and the counterface also increases. This elevated pressure causes plastic deformation of the softer aluminum matrix, which makes the material more susceptible to wear. Higher loads exacerbate wear mechanisms such as adhesive wear, where the material is transferred from the matrix to the counterface, and abrasive wear, where harder particles from the composite or counterface cause surface scratching [30]. At higher loads, a MML can form on the surface. This layer consists of wear debris and matrix material, which can temporarily protect the composite surface from further wear by acting as a buffer against the sliding surface. The formation of the MML helps reduce wear by distributing the applied forces over a larger area and reducing direct contact between the counterface and the matrix. However, this protection is temporary. As the load increases further, the MML can break down to the higher forces acting on it, exposing the softer matrix once again and leading to increased wear. This is evident from the slight decrease in wear rate observed as the load increases beyond 40 N, where the MML may have reached its capacity to protect the surface. The effect on friction is also notable. As the applied load increases, the friction coefficient may initially decrease, to the formation of a smoother surface or the stabilization of the MML. This could reduce the energy dissipated during sliding and momentarily lower the wear rate. However, when the load exceeds a certain threshold, the MML begins to break down, leading to more direct contact between the matrix and counterface. This breakdown increases friction and results in more abrasive interactions, thus elevating the wear rate

The heat generation and softening of the matrix at higher sliding velocities. As the velocity increases, the frictional heat produced at the interface between the composite and the counterface also rises. This heat softens the aluminum matrix, making it more prone to plastic deformation. The softened matrix loses its ability to firmly hold the reinforcement particles, causing them to become

dislodged more easily. As these reinforcement particles detach, the material undergoes more severe wear mechanisms, such as abrasive and adhesive wear, which increases the wear rate. This phenomenon is particularly pronounced at higher velocities, where the heat generated exceeds the matrix's ability to resist thermal degradation. The threshold effect observed in the results can be attributed to the initial reduction in wear rate with moderate increases in velocity [32]. At lower to moderate sliding speeds, the formation of a smoother surface or the stabilization of a MML may temporarily reduce wear by distributing the applied forces more evenly across the surface. However, as velocity exceeds a certain threshold, the heat generated becomes excessive, leading to accelerated matrix softening, more pronounced oxidation, and eventually a rapid increase in wear rate. A slight increase in wear rate was observed at higher velocities, particularly beyond 8 m/s. Increased debris production is another significant factor contributing to the increase in wear rate at higher velocities. The higher sliding speeds result in finer, more abrasive wear debris. This debris can act as a "third body" between the sliding surfaces, causing additional wear as it becomes trapped between the composite and the counterface. The finer debris is more abrasive and accelerates surface damage by scratching and cutting into the matrix. As velocity increases, the production of such debris intensifies, leading to more severe abrasive wear.

As the sliding distance increases, protective layers MML films on the composite surface gradually wear away. These protective layers serve to shield the underlying aluminum matrix from direct contact with the counterface. As they erode over longer distances, the softer aluminum matrix becomes exposed to greater frictional forces, leading to more severe wear. The continuous degradation of the surface thus results in a higher wear rate, as the material becomes more susceptible to damage from both abrasive and adhesive wear mechanisms. Another contributing factor is the increased debris accumulation over longer sliding distances. As the composite material undergoes wear, wear debris is generated. Over extended sliding distances, this debris can accumulate between the sliding surfaces, acting as an abrasive medium. This debris, especially if it is fine and hard, can significantly accelerate wear by scratching and gouging the surface of the aluminum matrix. The longer the distance, the more debris is produced and trapped between the surfaces, leading to higher wear rates. Also, in the progression of wear patterns Initially, wear may be dominated by mild adhesive wear, where material is transferred between the composite and the counterface. However, as the sliding distance increases, deeper grooves, scratches, and more severe abrasive wear develop. This progression occurs as the matrix becomes increasingly exposed and the wear debris acts as an abrasive agent, deepening the surface damage. The wear mechanisms evolve from less severe forms to more aggressive abrasive wear as the material undergoes continuous friction over a longer period.

3.5. Wear rate-lubricated

The reinforcement percentage of SiC and Gr particles in the aluminum matrix composite increases, and a

noticeable reduction in wear rate occurs, indicating enhanced wear resistance as depicted in Fig. 6.

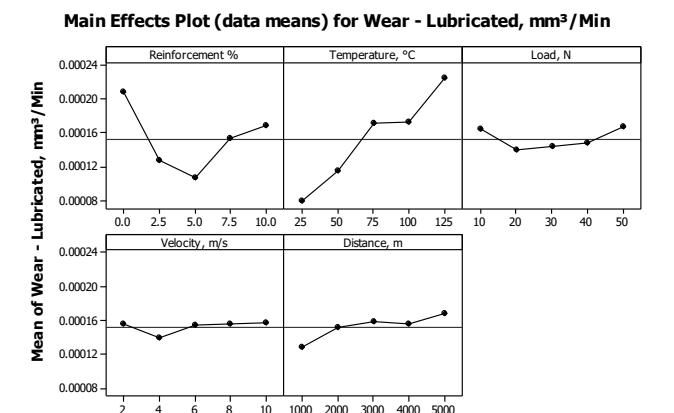


Fig. 6. The variation of wear rate in lubricated condition

The lowest wear rate, observed at a 5.0 % reinforcement level, underscores the optimal reinforcement proportion for wear resistance, beyond which a slight increase in wear rate occurs. This is primarily attributed to the enhanced wear resistance imparted by the incorporation of hard ceramic particles such as SiC and Gr within the aluminum matrix. The presence of these hard particles contributes to a robust load-bearing layer within the aluminum matrix, significantly reducing material deformation and wear. These particles, acting as micro-scale reinforcements, enhance the hardness of the composite material and limit surface deterioration during sliding contact. In lubricated conditions, engine oil theatres stabilize the effectiveness of these reinforcements [33]. The oil forms a tribofilm a protective film on the surface of the material which further embeds the SiC and Gr particles, ensuring consistent wear protection. The lubrication provided by the oil reduces friction and evenly distributes the particles across the interface, preventing the formation of agglomerates that could otherwise accelerate wear through abrasive mechanisms. Engine oil contributes to the stability of the composite by maintaining a well-dispersed distribution of reinforcing particles on the sliding surface, which is essential in reducing abrasive wear. In the absence of lubrication, as in dry conditions, the particles are more prone to agglomeration, which can lead to increased wear rates. This aggregation compromises the uniformity of the wearresistant surface layer, resulting in localized wear points and higher overall material loss. The synergistic effect of lubricant-induced film stability and the inherent hardness of SiC and Gr particles accounts for the reduction in wear rate [34]. The lubricating film lowers surface friction, minimizes direct contact between the sliding surfaces, and preserves distribution, effectively particle mitigating Consequently, the wear rate is significantly reduced in lubricated conditions compared to dry sliding, highlighting the beneficial impact of both particle reinforcement and lubrication on the wear resistance of the aluminum matrix composite.

The Gr particles embedded within the matrix provide a measure of thermal stability, reducing temperature-induced wear by forming a more thermally stable layer that counteracts softening. Additionally, the composite benefits from the dissipation of heat facilitated by engine oil, which acts as a cooling medium by carrying heat away from the wear interface. This cooling effect of the lubricant helps maintain the integrity of the aluminum matrix, preventing it from reaching temperatures at which severe softening and excessive wear would otherwise occur. Engine oil not only aids in heat dissipation but also forms a stable lubricating film across the sliding surfaces, which remains intact even at higher temperatures. This film reduces metal-to-metal contact and minimizes friction, protecting the surface from direct thermal exposure [35]. The SiC and Gr particles embedded within this lubricating layer further reinforce the wear-resistant properties by creating a durable barrier against wear. At elevated temperatures, these particles embedded within the tribofilm maintain their effectiveness, shielding the surface from abrasion and reducing the impact of increased thermal activity. The combined effects of thermal stability from Gr particles, heat dissipation provided by engine oil, and the stable lubricant film, reinforced with SiC and Gr particles, help stabilize the wear rate as temperature increases. These factors prevent a sharp increase in wear, indicating that the wear resistance of the composite under lubricated conditions is sustained more effectively than it would be in dry, unlubricated conditions. The gradual increase in wear rate with temperature under lubrication reflects the material's effective resilience against temperature-induced wear, largely to the synergistic roles of particle reinforcement and engine oil lubrication.

Under lubricated conditions, engine oil forms a cushioning layer that distributes the applied load more evenly across the contact surface, thus reducing localized stresses. This mixed lubrication regime allows for a smoother interaction between the surfaces and minimizes wear. The embedded SiC and Gr particles in the tribofilm serve as robust load-bearing agents, which help maintain structural integrity and reduce wear by supporting a significant portion of the load. The hard particles mitigate direct metal-to-metal contact, thus stabilizing the wear rate even under higher loading conditions. The presence of engine oil as a lubricant in preventing the detachment of reinforcement particles from the matrix [36]. At higher loads, there is a greater risk of particle pull-out to the increased shear stresses at the interface. However, the lubricating film formed by the engine oil keeps the SiC and Gr particles firmly embedded within the matrix, reducing the likelihood of particle detachment. This embedded particle stability is essential in minimizing abrasive wear, as detached particles could otherwise act as third-body abrasives and contribute to a higher wear rate. Another significant factor in maintaining a stable wear rate is the efficient debris removal facilitated by engine oil. As load increases, wear debris generation also tends to rise, which can lead to third-body abrasion if not effectively managed. The lubricant continuously removes wear debris from the contact interface, preventing it from accumulating and causing additional abrasive wear. This debris removal effect is especially critical under high-load conditions, where trapped particles could otherwise exacerbate wear by increasing friction and contributing to surface damage.

With this stability in wear rate the composite's wear resistance is effectively maintained even as velocity increases, largely to the presence of engine oil and the reinforcing particles embedded within the matrix. The nearly constant wear rate reflects the balance between lubrication and heat dissipation provided by the engine oil, which is essential in mitigating velocity-related wear impacts. At moderate velocities, the engine oil forms a stable lubricating film across the sliding surface. This film effectively minimizes friction by reducing direct contact between surfaces and leveraging the hardness of embedded SiC and Gr particles. These particles reinforce the tribofilm, enabling the composite to handle moderate velocities without succumbing to abrasive wear. This optimized film formation ensures that the composite experiences minimal wear even as sliding speed increases, with the lubricating film serving as a buffer that dampens surface interaction forces. As sliding velocity increases, the frictional heating effect typically intensifies, which would usually lead to an increase in wear rate. However, the cooling properties of engine oil counteract this heating, dissipating excess heat from the interface and reducing the risk of surface overheating. This cooling effect prevents the softening of the aluminum matrix, preserving the structural integrity of the composite even at higher velocities. Gr particles, known for their thermal stability, further resist temperature-induced wear, providing an additional layer of protection that enhances the composite's resilience at elevated sliding speeds. Together, the thermal stability of Gr and the cooling effect of engine oil ensure that wear rate remains stable and low, mitigating the adverse effects of increased velocity. In addition, engine oil controlling the movement and distribution of reinforcing particles within the tribofilm [37]. Under lubricated conditions, particles such as SiC and Gr remain embedded in the lubricating layer rather than becoming loose within the interface, where they could act as third-body abrasives. This retention of particles within the oil film is vital to maintaining a stable wear rate across different velocities, as loose particles in dry conditions would otherwise contribute to significant abrasive wear. The lubricant's ability to keep particles evenly dispersed and embedded in the tribofilm effectively prevents abrasive interactions that could increase the wear rate, allowing the composite to sustain wear resistance across the velocity spectrum.

Wear higher to surface roughness and initial adjustments as the surfaces come into contact. However, with the presence of engine oil, a stable tribofilm layer forms relatively quickly. This tribofilm, comprising both the lubricant and reinforcing particles such as SiC and Gr, reduces direct contact between the surfaces and protects against accelerated wear. By establishing a consistent boundary layer, the tribofilm stabilizes the wear rate across longer distances, providing an effective buffer that mitigates material removal and reduces wear variability as sliding progresses. Engine oil's continuous role in maintaining long-term durability is essential to sustaining a low wear rate over extended distances. As sliding continues, the oil replenishes the tribofilm layer, ensuring a stable protective film that shields the surface from both adhesive and abrasive wear mechanisms. This stable lubricating layer helps to evenly distribute the reinforcing particles across the contact area, enhancing the wear resistance of the composite by preventing localized stress concentrations. The tribofilm sustains a relatively consistent wear rate, despite the prolonged sliding distance, by reducing friction and enabling the reinforcement particles to continue functioning as load-bearing elements. The engine oil facilitates efficient debris control, which is particularly important for maintaining a stable wear rate over long distances. Wear debris generated during sliding is continuously removed from the contact interface by the oil, preventing it from accumulating and causing additional abrasive damage. In dry conditions, accumulated debris would act as third-body abrasives, significantly increasing wear. However, the lubricating oil prevents this effect, ensuring that abrasive wear is minimized and that the reinforcing particles retain their effectiveness throughout extended sliding distances. By actively removing debris, engine oil helps maintain a steady wear rate, allowing the composite material to sustain its wear resistance over time. In conclusion, the reduction of wear rate with increasing reinforcement content (up to 7.5% SiC-Gr) can be attributed to the load-bearing ability of SiC and the self-lubricating nature of Gr. SiC particles distribute stresses effectively, reducing plastic deformation, while Gr forms a tribo-film that minimizes direct metal-to-metal contact. However, at 10% reinforcement, particle agglomeration disrupts uniform load transfer, leading to localized stress concentrations and increased wear.

3.6. SEM analysis

In Fig. 7 a, the presence of micro-cracks and fracture patterns is prominently observed across the wear surface. These micro-cracks signify localized stress concentrations resulting from direct metal-to-metal contact, which is typical of abrasive wear mechanisms. The absence of a lubricating layer intensifies friction, leading to material fatigue and eventual fragmentation. Such cracks and fracture zones illustrate the composite's vulnerability to dry conditions, where repeated sliding promotes crack propagation and surface breakdown. Grooves and ploughing marks are also evident in Fig. 7 a, aligned with the sliding direction, which indicates the continuous abrasion caused by hard asperities or embedded particles. These linear grooves highlight the abrasive interactions between the counter surface and the aluminum matrix, where hard particles or surface asperities repeatedly cut into the material [38]. This ploughing effect illustrates how the material undergoes deformation and removal, a hallmark of abrasive wear under unlubricated conditions. In Fig. 7 b, wear debris formation is more noticeable, with clusters of loose particles accumulating on the surface. This debris likely originates from the detached fragments formed by micro-cracking and ploughing effects. The debris particles can act as a third body at the interface, exacerbating the wear process by generating additional abrasion and even embedding into the softer aluminum matrix. phenomenon creates a feedback loop, where loose particles accelerate further material removal, increasing wear severity. Fig. 7 also reveal an oxide layer on the worn surface, indicative of oxidation due to elevated temperatures from frictional heating. This oxide layer appears brittle and fragmented, a typical behavior of aluminum composites under dry wear conditions. The thermal-oxidative environment promotes the formation of this brittle film, which easily cracks under sliding stress, generating more wear debris. The oxide layer's instability contributes further to the degradation, as it does not provide protective support and instead accelerates material loss. Finally, adhesive wear features such as smeared and sheared regions are observed, particularly in Fig. 7 b, where localized areas show evidence of material transfer. These adhesive wear characteristics occur under higher loads and temperatures, where localized bonding and shearing transfer material between the sliding surfaces [39]. This adhesive interaction creates patches of smeared material, highlighting the tendency of aluminum composites to undergo metal transfer in dry, high-stress conditions.

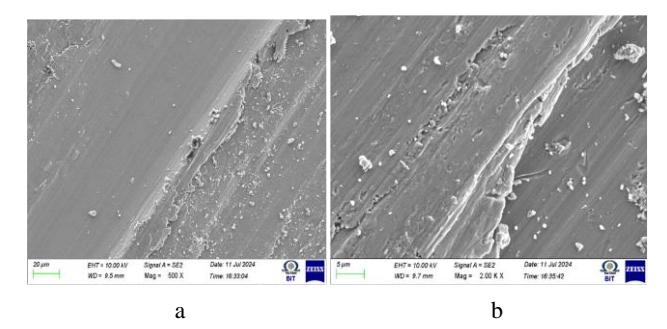


Fig. 7. Worn surface morphology of AA2024 composites under dry sliding condition: a – 500x; b – 2000x

In Fig. 8 a, a reduction in groove depth is evident, with the grooves appearing shallower and showing reduced ploughing marks compared to unlubricated wear conditions. This suggests that lubrication minimizes direct metal-tometal contact, thereby diminishing abrasive wear that would otherwise result in deep grooves and intense ploughing. The smoother surface finish observed in Fig. 8 b further aligns with this observation, as lubrication reduces friction during sliding, leading to less severe wear scars and scratch marks. The surface in lubricated conditions appears comparatively uniform, with fewer deformation features, indicating the lubricant's role in softening the sliding impact and limiting severe wear [40]. Additionally, Fig. 8 demonstrates a marked decrease in oxide formation on the lubricated surfaces. Under unlubricated conditions, friction often raises temperatures at contact points, which can lead to brittle oxide layer formation that exacerbates wear through the brittle fracture.

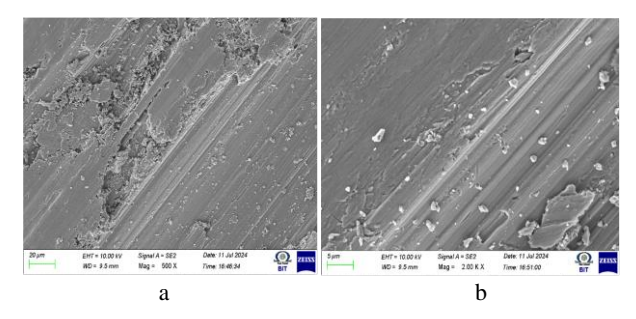


Fig. 8. Worn surface morphology of AA2024 composites under lubricating sliding condition: a – 500x; b – 2000x

However, the presence of lubrication reduces the operational temperature, thereby minimizing the likelihood of oxide layer formation. This absence of oxide layers in the lubricated conditions shown in the figures indicates a reduction in temperature-driven wear mechanisms,

contributing to the material's longevity under sliding conditions. A significant observation in Fig. 8 a is the presence of a transferred lubricant film on the wear surface in certain regions. This thin film acts as a protective barrier, reducing direct metal-to-metal contact and facilitating smoother sliding interactions. By filling micro-voids and surface asperities, the lubricant film further reduces abrasive impact and enhances the surface finish. This transferred film layer implies that the lubricant plays an active role in wear protection, creating a continuous buffer that limits direct surface degradation [41]. Compared to unlubricated conditions, the images reveal significantly less wear debris, the lubricant's ability to carry away particles generated during sliding. By removing debris from the contact area, the lubricant prevents these particles from contributing to abrasive wear, which would otherwise increase material removal and surface roughness [42]. This finding suggests that the lubricant enhances surface cleanliness, contributing to smoother interactions and extending the wear surface's lifespan. Adhesive wear, typically characterized by smearing and material transfer between surfaces, is minimized under lubricated conditions [43]. The defined boundaries between contact areas suggest that lubrication effectively prevents material adhesion, which can otherwise lead to severe material damage.

3.7. Wear equation

The wear equation for dry conditions, W_{dry} , can be defined as follows, with separate cases based on the values of relative humidity R and applied force F.

The developed wear equation for dry conditions predicts wear behavior under varying operating parameters. It was divided into two cases based on experimental results. For $R \le 7.5$ %, wear increases with Fe and Va but decreases with Rd, Db, and Tc. For R > 7.5 %, wear was primarily influenced by Rd and Db, with reduced dependence on Fe and Va. Empirical constants (C_1, C_2) and exponents (a, b, c, C_1) d, e) were determined to align with experimental data as shown in Eq. 1:

$$W_{dry} = \begin{cases} \frac{F_e \cdot V^a}{R^d \cdot C_1 \cdot D^b \cdot T^c}, & \text{if } R \le 7.5\% \text{ and } F \le 20\text{N} \\ \frac{R^f \cdot D^b}{F_e \cdot C_2 \cdot V^a \cdot T^c}, & \text{if } R > 7.5\% \text{ and } F > 20\text{N} \end{cases}, \tag{1}$$

where W_{dry} is the wear rate in dry conditions; $W_{lubricated}$ is the wear rate in lubricated conditions; L is the lubricant properties (possibly related to lubrication film thickness or viscosity): F_e is the applied load or force; V is the sliding velocity; R is the relative humidity; D is the distance or sliding distance; T is the temperature; a, b, c, d, and f are empirical exponents that account for the effects of each variable; C_1 and C_2 are material-specific constants for each

This derivative reveals the reinforcement affects wear under specific conditions. The negative exponent –(d+1) indicated an inverse relationship, meaning that as reinforcement increases, wear decreases at an accelerated rate. The magnitude of the change depends on the value of d, which quantifies the sensitivity of wear to reinforcement. For $R \le 7.5\%$ and $F \le 20N$

$$\frac{dW_{dry}}{dR} = \frac{F_e \cdot V^{a.d.} \cdot R^{-(d+1)}}{C_1 \cdot D^{b.T^c}}.$$
 (2)

When the percentage of reinforcement is above 7.5 %, reinforcement plays a dominant role in determining wear. The direct proportionality suggests that materials with higher reinforcement percentages can significantly enhance wear rate under high load and speed. Conversely, Fe, V, and temperature T appear in the denominator, indicating that higher values of these parameters increase the wear rate with respect to reinforcement as shown in Eq. 3.

For R > 7.5% and F > 20N

$$\frac{dW_{dry}}{dR} = \frac{f \cdot R^{(f-1)} \cdot D^b}{F_e \cdot C_2 \cdot V^a \cdot T^c}.$$
 (3)

As the LHS of the Eq. 2 and Eq. 3 was same, hence equating the RHS expressions as shown in Eq. 4

$$-\frac{F_e \cdot V^{a} \cdot d \cdot R^{-(d+1)}}{C_1 \cdot D^b \cdot T^c} = \frac{f \cdot R^{(f-1)} \cdot D^b}{F_e \cdot C_2 \cdot V^a \cdot T^c}.$$
 (4)

This will further be simplified to Eq. 5.

$$-\frac{d \cdot R^{-(d+1)}}{c_1} = \frac{f \cdot R^{(f-1)}}{c_2}.$$
 (5)

The work was intended to study the impact of reinforcement on wear rate hence the equation will be rewritten as per Eq. 6.

$$R = \left(\frac{f \cdot C_1}{d \cdot C_2}\right)^{\frac{1}{d+f}} \tag{6}$$

This is the expression for R in terms of the constants d, f, C_1 and C_2 .

The wear equation for lubricated conditions accounts for the effects of various factors on wear behavior. In case 1, wear is inversely proportional to applied force, sliding velocity, distance, and temperature, with reinforcement and lubrication enhancing wear resistance. The lubrication factor appears as a multiplier, signifying its critical role in reducing wear by providing a protective film between surfaces. In case the wear was primarily influenced by reinforcement, with a stronger dependence on lubrication and load. Higher reinforcement reduces wear, while lubrication remains essential in reducing friction and wear under higher loads and velocities as depicted in Eq. 7.

For lubricated condition

$$W_{Lub} = \begin{cases} \frac{C_1 \cdot R^d \cdot L^g}{F_e \cdot V^a \cdot D^b \cdot T^c}, & \text{if } R \le 5\% \text{ and } F \le 20\text{N} \\ \frac{C_2 \cdot L^g}{F_e \cdot R^f \cdot V^a \cdot D^b \cdot T^c}, & \text{if } R > 5\% \text{ and } F > 20\text{N} \end{cases} . (7)$$

Now, we differentiate $W_{lubricated}$ with respect to R as depicted in Eq. 8 and Eq. 9.

$$\frac{dW_{lubricated}}{dR} = \left(\frac{c_1 \cdot L^g \cdot d \cdot R^{d-1}}{F_e \cdot V^a \cdot D^b \cdot T^c}\right); \tag{8}$$

$$\frac{dW_{lubricated}}{dR} = -\frac{c_2 \cdot f \cdot R^{-(f+1)} \cdot L^g}{F_e \cdot V^a \cdot D^b \cdot T^c}.$$
 (9)

Similarly as calculated for dry condition, R was calculated for wet condition as depicted in Eq. 10.

$$R = \left(-\frac{c_2 \cdot f}{c_1 \cdot d}\right)^{\frac{1}{f - d + 2}} \tag{10}$$

Followed by the Eq. 7 and Eq. 11 were equated. As equating as the factor $L_{\rm g}$ was not present in equation 7, it was added to Eq. 10 to study the impact of lubrication, and it was expressed as Eq. 11.

$$L_g = \frac{R_2}{R_1} = \frac{\left(-\frac{C_2 \cdot f}{C_1 \cdot d}\right)^{\frac{1}{f - d + 2}}}{\left(\frac{f \cdot C_1}{d \cdot C_2}\right)^{\frac{1}{d + f}}}.$$
 (11)

The equation was further simplified to Eq. 12. The expression Lg provides valuable insight of the lubrication properties and it was influenced by various material parameters.

$$L_g = \left(-\frac{C_2 \cdot f}{C_1 \cdot d}\right)^{\frac{1}{f - d + 2}} \times \left(\frac{f}{d}\right)^{\frac{1}{d + f}} \times \left(\frac{C_1}{C_2}\right)^{\frac{1}{d + f}}.$$
 (12)

The constants C_1 and C_2 , along with the factors f and d, interacted in a complex manner to determine lubrication effectiveness. These parameters were critical in understanding the lubrication behavior under different conditions, including reinforcement percentage and applied load. The equation for L_g highlights the relationship between these factors and emphasizes their influence on wear resistance in tribological systems. The interplay between C_1 , C_2 , f, and d governs the performance of lubricants in reducing friction and wear.

4. CONCLUSIONS

Reinforcements (SiC and Gr) were uniformly distributed within the aluminum matrix, with no visible agglomeration, as revealed by SEM. Good bonding between the matrix and reinforcement phases was observed, ensuring consistent mechanical properties and effective load distribution. A consistent increase in hardness was noted with higher reinforcement percentages, reaching a peak at 10 % reinforcement. The increase was attributed to the dispersion hardening mechanism, wherein the harder ceramic particles inhibited dislocation enhancing resistance to deformation. Tensile strength improved with an increase in reinforcement content due to the strong interfacial bonding between the matrix and the particles. The improvement plateaued beyond 7.5 % reinforcement due to potential particle agglomeration, which reduced the strengthening effect.

Wear rate decreased significantly with increasing reinforcement content, attributed to the hardness and load-bearing capacity imparted by the SiC and Gr particles. At higher loads and sliding velocities, wear mechanisms shifted from severe adhesive wear to controlled mild abrasive wear due to the formation of mechanically mixed layers. Oxidation effects became prominent at elevated temperatures, forming brittle oxide layers that contributed to wear debris and accelerated material loss.

The addition of engine oil reduced the wear rate significantly across all reinforcement levels. The optimal wear resistance was observed at 5 % reinforcement, attributed to the synergistic effect of lubrication and reinforcement particles. Lubrication stabilized particle distribution, minimized friction, and prevented material softening by dissipating frictional heat. At moderate sliding velocities, a stable tribofilm reduced wear, while at higher

velocities, frictional heat increased wear due to thermal softening of the aluminum matrix. Longer sliding distances led to gradual erosion of protective layers, exposing the softer matrix and increasing wear rates, though lubrication significantly mitigated this effect.

Under dry conditions, SEM analysis showed microcracks, grooves, and abrasive wear features, with evidence of brittle oxide layers exacerbating material loss. Lubricated surfaces exhibited shallower grooves, reduced ploughing, and smoother finishes, indicating the effectiveness of lubrication in reducing wear severity. Dry conditions resulted in higher debris generation, which acted as third-body abrasives, accelerating wear. In lubricated conditions, debris was effectively removed by the lubricant, preventing abrasive interactions and maintaining low wear rates. Gr particles contributed to thermal stability, mitigating the effects of frictional heat and reducing temperature-induced wear. Engine oil acted as a cooling medium, dissipating heat and maintaining the integrity of the composite under higher sliding velocities and loads.

Empirical wear equations were developed for both dry and lubricated conditions, accurately predicting wear rates based on reinforcement percentage, applied load, sliding velocity, and temperature. The equations reveal that reinforcement significantly reduces wear, while lubrication further enhances wear resistance by forming a protective film.

5. SCOPE FOR FUTURE WORK

Machine learning models can be developed utilizing the refined empirical wear equations by incorporating dynamic wear progression. Validation through industrial-scale tribological testing will be done to evaluate performance under industrial operating conditions.

REFERENCES

- Srivyas, P.D., Charoo, M.S. Tribological Behavior of Hybrid Aluminum Self-Lubricating Composites Under Dry Sliding Conditions at Elevated Temperature Tribology-Materials, Surfaces & Interfaces 16 (2) 2022: pp. 153-167. https://doi.org/10.1080/17515831.2021.1931771
- Kumar, K., Davim, J.P. Biodegradable Composites: Materials, Manufacturing and Engineering. Walter de Gruyter GmbH & Co KG. 2019.
- Mohan, S., Pathak, J.P., Gupta, R.C., Srivastava, S. Wear Behaviour of Graphitic Aluminium Composite Sliding Under Dry Conditions *International Journal of Materials Research* 93 (12) 2022: pp. 1245 – 1251. https://doi.org/10.1515/ijmr-2002-0214
- Martin, S., Kandemir, S., Antonov, M. Investigation of The High Temperature Dry Sliding Wear Behavior of Graphene Nanoplatelets Reinforced Aluminum Matrix Composites Journal of Composite Materials 55 (13) 2021: pp. 1769 – 1782. https://doi.org/10.1177/0021998320979037
- Jiménez, A.E., Bermúdez, M.D. Tribology for Engineers – A Practical Guide. Woodhead: Sawston, UK. 2011
- Srivyas, P.D., Charoo, M.S. Friction and Wear Characterization of Spark Plasma Sintered Hybrid Aluminum

- Composite Under Different Sliding Conditions *Journal of Tribology* 142 (12) 2020: pp. 121–701. https://doi.org/10.1115/1.4047456
- Zhang, P., Zeng, L., Mi, X., Lu, Y., Luo, S., Zhai, W. Comparative Study on the Fretting Wear Property of 7075 Aluminum Alloys Under Lubricated and Dry Conditions Wear 474 2021: pp. 203 760. https://doi.org/10.1016/j.wear.2021.203760
- Davim, J.P. Wear of Advanced Materials. John Wiley & Sons. 2013.
- Mercado-Lemus, V.H., Gomez-Esparza, C.D., Díaz-Guillén, J.C., Mayén-Chaires, J., Gallegos-Melgar, A., Arcos-Gutierrez, H., Perez-Bustamante, R. Wear Dry Behavior of the Al-6061-Al2O3 Composite Synthesized by Mechanical Alloying *Metals* 11 (10) 2021: pp. 1652. https://doi.org/10.3390/met11101652
- Wang, Y., Zhang, J. A Review of the Friction and Wear Behavior of Particle-Reinforced Aluminum Matrix Composites *Lubricants* 11 (8) 2023: pp. 317. https://doi.org/10.3390/lubricants11080317
- Mercado-Lemus, V.H., Gomez-Esparza, C.D., Díaz-Guillén, J.C., Mayén-Chaires, J., Gallegos-Melgar, A., Arcos-Gutierrez, H. Perez-Bustamante, R. Wear Dry Behavior of the Al-6061-Al2O3 Composite Synthesized by Mechanical Alloying *Metals* 11 (10) 2021: pp. 1652. https://doi.org/10.3390/met11101652
- Khelge, S., Kumar, V., Shetty, V., Kumaraswamy, J. Effect of Reinforcement Particles on the Mechanical and Wear Properties of Aluminium Alloy Composites: Review *Materials Today: Proceedings* 52 2022: pp. 571 576. https://doi.org/10.1016/j.matpr.2021.09.525
- Khan, M.M., Hajam, M.I., Mir, Z.A. Optimizing the Effect of Solid Lubricants on the Sliding Wear Behavior of SiCp Reinforced Cast Aluminum Alloy *Journal of Bio-and Tribo-Corrosion* 7 (1) 2021: pp. 23. https://doi.org/10.1007/s40735-020-00460-w
- 14. Jayapragash, A., Solamannan, G.G., Guganeswaran, I. Influence of Corrosion Behaviour on Lm4/Zro2 Metal Matrix Composites In IOP Conference Series: Materials Science and Engineering 912 (5) 2020: pp. 052008. https://doi.org/10.1007/s40735-020-00460-w
- 15. Saravanakumar, A., Bhuvaneswari, V., Gokul, G. Optimization of Wear Behaviour for AA2219-Mos2 Metal Matrix Composites in Dry and Lubricated Condition Materials Today: Proceedings 27 2020: pp. 2645 2649. https://doi.org/10.1016/j.matpr.2019.11.087
- 16. Shinde, D.M., Poria, S., Sahoo, P. Dry Sliding Wear Behavior of Ultrasonic Stir Cast Boron Carbide Reinforced Aluminium Nanocomposites Surface Topography: Metrology and Properties 8 (2) 2020: pp. 025033. https://doi.org/10.1088/2051-672X/ab9d71
- 17. Kumar, P.S., Sachit, T.S., Mohan, N., Akshay Prasad, M. Dry Sliding Wear Behaviour of Al-5Si-3Cu-0.5Mn Alloy and Its WC Reinforced Composites at Elevated Temperatures *Materials Today: Proceedings* 44 2021: pp. 566–572. https://doi.org/10.1016/j.matpr.2020.10.351
- Joseph, J.D., Kumaragurubaran, B., Sathish, S. Effect of MoS₂ on the Wear Behavior of Aluminium (AlMg0.5Si) Composite Silicon 12 (6) 2020: pp. 1481 – 1489. https://doi.org/10.1007/s12633-019-00238-x
- Bharath, V., Auradi, V., Nagaral, M., Boppana, S.B., Ramesh, S., Palanikumar, K. Microstructural and Wear Behavior of Al2014-Alumina Composites with Varying Alumina Content *Transactions of the Indian Institute of Metals* 2022: pp. 1-15.

- https://doi.org/10.1007/s12666-021-02405-4
- Güney, B., Mutlu, İ. Wear and Corrosion Resistance of Cr2O3%-40%Tio2 Coating on Gray Cast-Iron by Plasma Spray Technique Materials Research Express 6 (9) 2019: pp. 096577. https://doi.org/10.1088/2053-1591/ab2fb7
- Hasan, M.S., Kordijazi, A., Rohatgi, P.K., Nosonovsky, M. Triboinformatic Modeling of Dry Friction and Wear of Aluminum Base Alloys Using Machine Learning Algorithms *Tribology International* 161 2021: pp. 107065. https://doi.org/10.1016/j.triboint.2021.107065
- Kumar, D., Angra, S., Singh, S. High-Temperature Dry Sliding Wear Behavior of Hybrid Aluminum Composite Reinforced with Ceria and Graphene Nanoparticles Engineering Failure Analysis 151 2023: pp. 107426. https://doi.org/10.1016/j.engfailanal.2023.107426
- Srivyas, P.D., Charoo, M.S. Tribological Behavior of Aluminum Silicon Eutectic Alloy Based Composites Under Dry and Wet Sliding for Variable Load and Sliding Distance SN Applied Sciences 2 (10) 2020: pp. 1654. https://doi.org/10.1007/s42452-020-03433-3
- 24. Samal, P., Mandava, R.K., Vundavilli, P.R. Dry Sliding Wear Behavior of Al 6082 Metal Matrix Composites Reinforced with Red Mud Particles SN Applied Sciences 2 (2) 2020: pp. 313. https://doi.org/10.1007/s42452-020-2136-2
- 25. **Davim, J.P.** Materials and Surface Engineering: Research and Development. Elsevier, 2012.
- Sachit, T.S., Mohan, N., Suresh, R., Prasad, M.A.
 Optimisation of Dry Sliding Wear Behaviour of Aluminum LM4-Ta/Nbc Nano Composite Using Taguchi Technique Materials Today: Proceedings 27 2020: pp. 1977 1983. https://doi.org/10.1016/j.matpr.2019.09.043
- Dinaharan, I., Gladston, J.A.K., Selvam, J.D.R., Jen, T.C. Influence of Particle Content and Temperature on Dry Sliding Wear Behaviour of Rice Husk Ash Reinforced AA6061 Slurry Cast Aluminum Matrix Composites Tribology International 183 2023: pp. 108406. https://doi.org/10.1016/j.triboint.2023.108406
- 28. **Ashwath, P., Xavior, M.A.** Dry Sliding Wear Behaviour of T6-Aluminium Alloy Composites Compared with Existing Aircraft Brake Pads *Arabian Journal for Science and Engineering* 46 (12) 2021: pp. 11971 11984. https://doi.org/10.1007/s13369-021-05770-w
- 29. **Saessi, M., Alizadeh, A., Abdollahi, A.** Wear Behavior and Dry Sliding Tribological Properties of Ultra-Fine Grained Al5083 Alloy and Boron Carbide-Reinforced Al5083-Based Composite at Room and Elevated Temperatures *Transactions of Nonferrous Metals Society of China* 31 (1) 2021: pp. 74–91. https://doi.org/10.1016/S1003-6326(20)65479-6
- Murugabalaji, V., Rout, M., Sahoo, B.N. Wear Behaviour Analysis of Thermo-Mechanically Processed AA7075 and AA7075/Sic/Graphite Composite *Materials Chemistry and Physics* 327 2024: pp. 129890. https://doi.org/10.1016/j.matchemphys.2024.129890
- 31. **Güney, B., Mutlu, I.** Tribological Properties Of Brake Discs Coated With Cr2o3–40% Tio2 By Plasma Spraying *Surface Review and Letters* 26 (10) 2019: pp. 1950075. https://doi.org/10.1142/S0218625X19500756
- 32. **Davim, J.P.** Composite Materials: A Bibliometric Analysis *AIMS Materials Science* 11 (6) 2024: pp. 1145–1148. https://doi.org/10.3934/matersci.2024055

- 33. Ravinath, H., Ahammed, I., Harigovind, P.V.R.A.S., VR, A.S., Shankar, K.V., Nandakishor, S. Impact of Aging Temperature on the Metallurgical and Dry Sliding Wear Behaviour of LM25 / Al₂O₃ Metal Matrix Composite for Potential Automotive Application International Journal of Lightweight Materials and Manufacture 6 (3) 2023: pp. 416–433. https://doi.org/10.1016/j.ijlmm.2023.01.002
- 34. **Vithal, N.D., Krishna, B.B., Krishna, M.G.** Impact of Dry Sliding Wear Parameters on the Wear Rate of A7075 Based Composites Reinforced with Zrb2 Particulates *Journal of Materials Research and Technology* 14 2021: pp. 174–185. https://doi.org/10.1016/j.jmrt.2021.06.005
- 35. **Kasar, A.K., Menezes, P.L.** Friction and Wear Behavior of Alumina Composites with In-Situ Formation Of Aluminum Borate And Boron Nitride *Materials* 13 (20) 2020: pp. 4502. https://doi.org/10.3390/ma13204502
- 36. Kirubakaran, J., Divahar, S.R., Dhas, J.E.R., Lewise, K.A.S., Anand, A.V. Wear Behavior Analysis of Aluminium Composites Using Taguchi Approach *Materials Today: Proceedings* 64 2022: pp. 345–351. https://doi.org/10.1016/j.matpr.2022.04.694
- Rajesh, K., Mahendra, K.V., Mohan, N., Sachit, T.S., Akshay Prasad, M. Studies on Mechanical and Dry Sliding Wear Behaviour of Graphite/Flyash Reinforced Aluminium (Al6Mg) MMCS Materials Today: Proceedings 27 2020: pp. 2434 2440. https://doi.org/10.1016/j.matpr.2019.09.211

- 38. Sharath, B.N., Venkatesh, C.V., Afzal, A., Baig, M.A.A., Kumar, A.P. Study on Effect of Ceramics on Dry Sliding Wear Behaviour of Al-Cu-Mg Based Metal Matrix Composite at Different Temperature *Materials Today: Proceedings* 46 2021: pp. 8723 8733. https://doi.org/10.1016/j.matpr.2021.04.034
- 39. Luo, Y., Xue, S., Mei, H., Wang, H., Weng, H., Mao, Y., Cao, J. Investigation of Tribology and Life Prediction of Polymer Coatings on 7N21 Aluminum Alloy Under Dry Sliding Wear *Colloids and Surfaces A: Physicochemical and Engineering Aspects* 703 2024: pp. 135384. https://doi.org/10.1016/j.colsurfa.2024.135384
- 40. **Patel, M., Sahu, S.K., Singh, M.K., Kumar, A.** Sliding Wear Behavior of Particulate Reinforced Aluminium Metal Matrix Composites *International Journal of Engineering Research in Current Trends* 2 (3) 2020: pp. 8–13.
- 41. **Kumar, P.S.R., Mashinini, P.M.** Dry Sliding Wear Behaviour of AA7075 Al2SiO5 Layered Nanoparticle Material at Different Temperature Condition *Silicon* 13 (12) 2021: pp. 4259–4274. https://doi.org/10.1007/s12633-020-00728-3
- 42. **Kılıç, H., Güney, B.** Investigation on Tribo-Properties of Twaron Pulp-Reinforced Brake Friction Composites *Polymer Composites* 46 (1) 2025: pp. 949-962. https://doi.org/10.1002/pc.29274
- 43. Tankal, K., Güney, B., Erden, M.A. A Comparative Study of Thermal Sprayed Al2O3-Tio2 Coatings On PM AISI 316L Engineering Science and Technology, an International Journal 60 2024: pp. 101895. https://doi.org/10.1016/j.jestch.2024.101895



© Maddi et al. 2025 Open Access This article is distributed under the terms of the Creative Commons Attribution 4.0 International License (http://creativecommons.org/licenses/by/4.0/), which permits unrestricted use, distribution, and reproduction in any medium, provided you give appropriate credit to the original author(s) and the source, provide a link to the Creative Commons license, and indicate if changes were made.